Atmospheric Environment 180 (2018) 37–50

Contents lists available at ScienceDirect

Atmospheric Environment

journal homepage: www.elsevier.com/locate/atmosenv

Long-term aerosol climatology over Indo-Gangetic Plain: Trend, prediction and potential source fields

M. Kumar[a], K.S. Parmar[b], D.B. Kumar[c], A. Mhawish[a], D.M. Broday[d], R.K. Mall[a,e], T. Banerjee[a,e,*]

[a] Institute of Environment and Sustainable Development, Banaras Hindu University, Varanasi, India
[b] Department of Mathematics, Punjab Technical University, Jalandhar, Kapurthala, India
[c] School of Civil Engineering, Kalinga Institute of Industrial Technology University, Bhubaneswar, India
[d] Civil and Environmental Engineering, Technion, Haifa, Israel
[e] DST-Mahamana Centre of Excellence in Climate Change Research, Banaras Hindu University, Varanasi, India

GRAPHICAL ABSTRACT

Decadal (2006–2015) variation of averaged AOD and Angstrom Exponent over IGP.

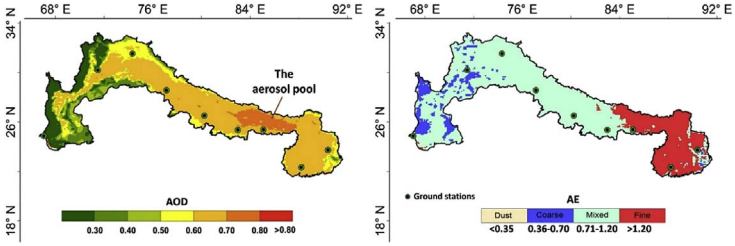

Decadal (2006-2015) variation of averaged AOD and Angstrom Exponent over IGP.

ARTICLE INFO

Keywords:
ARIMA
AOD
Fine particulates
MODIS
Spatiotemporal comparison
Trend

ABSTRACT

Long-term aerosol climatology is derived using Terra MODIS (Collection 6) enhanced Deep Blue (DB) AOD retrieval algorithm to investigate decadal trend (2006–2015) in columnar aerosol loading, future scenarios and potential source fields over the Indo-Gangetic Plain (IGP), South Asia. Satellite based aerosol climatology was analyzed in two contexts: for the entire IGP considering area weighted mean AOD and for nine individual stations located at upper (Karachi, Multan, Lahore), central (Delhi, Kanpur, Varanasi, Patna) and lower IGP (Kolkata, Dhaka). A comparatively high aerosol loading (AOD: 0.50 ± 0.25) was evident over IGP with a statistically insignificant increasing trend of 0.002 year^{-1}. Analysis highlights the existing spatial and temporal gradients in aerosol loading with stations over central IGP like Varanasi (decadal mean AOD ± SD; 0.67 ± 0.28) and Patna (0.65 ± 0.30) exhibit the highest AOD, followed by stations over lower IGP (Kolkata: 0.58 ± 0.21; Dhaka: 0.60 ± 0.24), with a statistically significant increasing trend (0.0174–0.0206 year^{-1}). In contrast, stations over upper IGP reveal a comparatively low aerosol loading, having an insignificant increasing trend. Variation in AOD across IGP is found to be mainly influenced by seasonality and topography. A distinct "aerosol pool" region over eastern part of Ganges plain is identified, where meteorology, topography, and aerosol sources favor the persistence of airborne particulates. A strong seasonality in aerosol loading and types is also witnessed, with high AOD and dominance of fine particulates over central to lower IGP, especially during post-monsoon and winter. The time series analyses by autoregressive integrated moving average (ARIMA) indicate contrasting patterns in randomness of AOD over individual stations with better performance especially over central IGP. Concentration weighted trajectory analyses identify the crucial contributions of western dry regions and partial contributions from central Highlands and north-eastern India, in regulating AOD over stations across IGP. Although our analyses provide some attributes to the observed changes in aerosol loading, we

* Corresponding author. Institute of Environment and Sustainable Development, Banaras Hindu University, Varanasi, 221005, India.
E-mail addresses: tb.iesd@bhu.ac.in, tirthankaronline@gmail.com (T. Banerjee).

https://doi.org/10.1016/j.atmosenv.2018.02.027
Received 23 December 2017; Received in revised form 11 February 2018; Accepted 12 February 2018
Available online 20 February 2018

conclude that the spatial and temporal pattern of aerosol properties is highly complex and dynamic over IGP, and require further investigation in order to reduce uncertainty in aerosol-climate model.

1. Introduction

Atmospheric aerosols are integral components of the earth's climatic system which directly or indirectly affect the Earth's energy budget and thereby, regulate the hydrological cycle and global food security. The climatic impacts of aerosols are mainly governed by its genesis, physio-chemical characteristics, spatio-temporal distribution, morphology and by the variation in its mixing states. Aerosols although impart significant influences on the climate system through its direct, indirect and semi-direct Aerosol-Radiation Interactions (ARI), the interaction of atmospheric aerosols with insolation (mainly within lower atmosphere) forms the primary basis of their climate governing properties. Aerosols significantly modify the global energy budget either directly through extinction of solar radiation (Schulz et al., 2006) or through influencing the cloud optical properties by behaving as cloud condensation nuclei (Seinfeld et al., 2016). Apart from its climate governing properties, aerosols are also crucial in terms of instigating poor air quality and thereby to affect human health (Evans et al., 2013; Kumar et al., 2015a), impair visibility (Han et al., 2012), regulate oxidative properties of atmosphere (Rastogi and Patel, 2017) and to reduce crop yield (Burney and Ramanathan, 2014).

The Indo-Gangetic Plain (IGP) of South Asia characteristically experiences massive and diverse aerosol burden due to multiple emission sources, unique location and topography, regional meteorology, socio-economic development and human behavior (Fig. 1, Banerjee et al., 2015, 2017; Singh et al., 2017a,b). The anthropogenic emission of fine particulates ($PM_{2.5}$) over South Asia, including IGP, have been recently documented by Singh et al. (2017a). The entire region is reported to experience considerable spatial and seasonal variations of particulate sources, with overall vehicular emissions to be the most dominating $PM_{2.5}$ source, followed by industrial emissions, secondary aerosols and natural sources. Natural aerosols like dust and sea salt, originate mainly from the western dry regions and nearby oceans are transported by the prevailing winds, thus contributing to regional aerosol loading (Kumar et al., 2015b; Sen et al., 2017). Seasonal variations in dominant aerosol sources and associated changes in aerosol physico-chemical and optical properties are the unique characteristics of IGP (Mhawish et al., 2017; Sen et al., 2016, 2017). However, the sparsely distributed monitoring network limits gaining fundamental understanding of aerosol sources, chemistry and dynamics. Comprehensive assessment of aerosol climatology, possible future trend along with their potential sources on spatial and temporal scales are therefore absolutely necessary to reduce uncertainties in aerosol-climate model.

Recent advancements in satellite based aerosol measurement have endowed the potentials to examine multiple aerosol properties over a relatively larger area with high number of repeated observation (Mhawish et al., 2018). MODerate resolution Imaging Spectro-radiometer (MODIS) on-board Terra and Aqua satellite has been widely exploited for various Earth and atmospheric applications, including air quality assessment (Kumar et al., 2016, 2017a,b, Sorek-Hamer et al.,

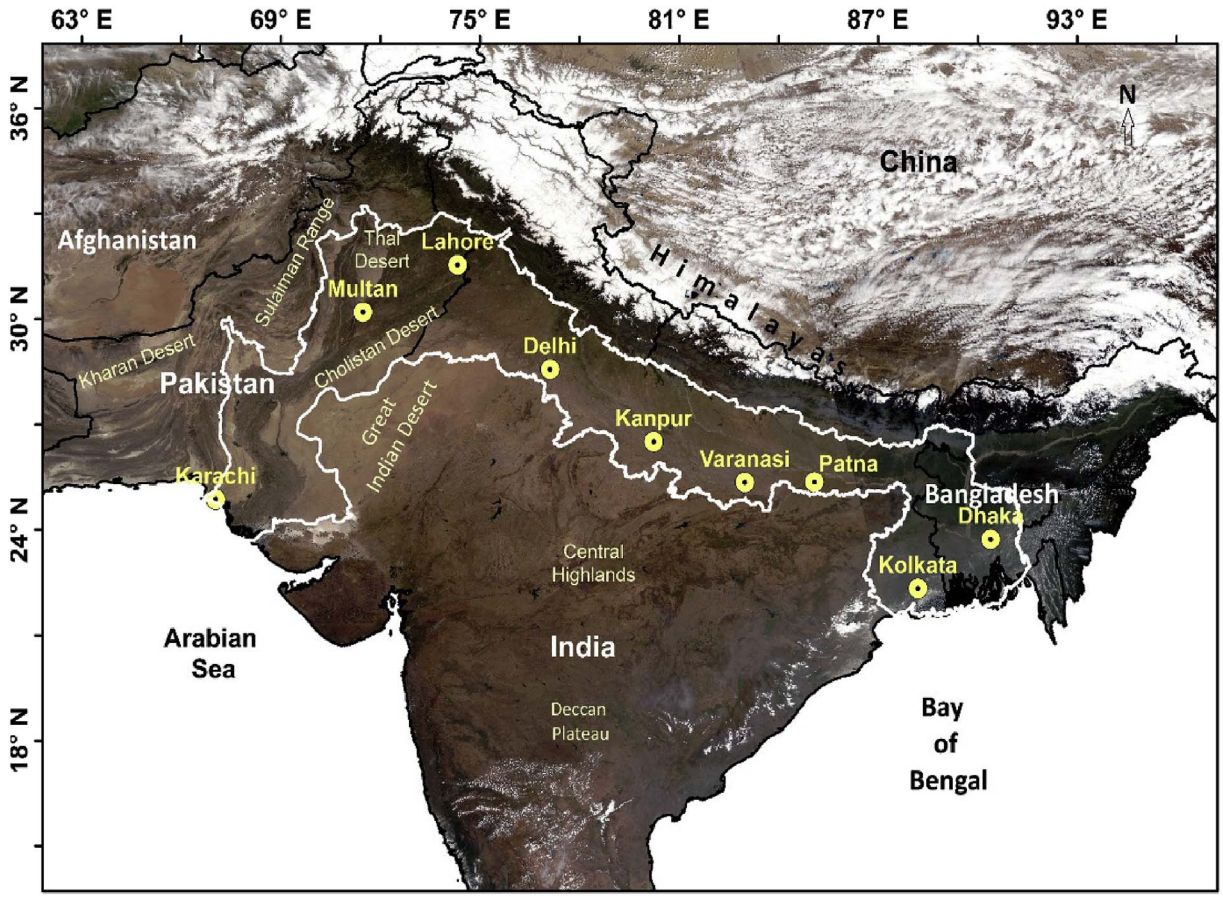

Fig. 1. MODIS true color image of the study region indicating all the nine stations across Indo-Gangetic Plain. (For interpretation of the references to color in this figure legend, the reader is referred to the Web version of this article.)

2015), long-term climatology (Soni et al., 2015), estimating surface-level particulate concentration (Sorek-Hamer et al., 2013a), exposure and mortality studies (Van Donkelaar et al., 2010), crop yield simulation (Fang et al., 2011), studying pollution episodes (Kumar et al., 2016; Sorek-Hamer et al., 2013b) and for forecasting of climate extremes (Dey et al., 2004). There are efforts to understand aerosol climatology and trend in columnar aerosol loading (Soni et al., 2015; Lodhi et al., 2013; Ramachandran et al., 2012). Time series analysis, like auto-regressive (AR) and moving average (MA) models along with their combinations, are also applied at various locations to study the long-term variability in aerosols.

The present work highlights the long-term aerosol climatology over IGP, considering satellite derived aerosol properties over nine stations. The current analysis has another advantage, since it utilizes the "second generation" Collection 6 (C6) enhanced Deep Blue (DB) algorithm over land, which has proven capability of retrieving AOD over arid/desert region, and improved assessment of NDVI-dependent surface reflectance, cloud screening and dust identification (Hsu et al., 2013). The MODIS C6 DB products have been previously well validated over different regions of the world (Wei et al., 2018; He et al., 2018; Bilal and Nichol, 2015; Tao et al., 2015) and especially over IGP (Mhawish et al., 2017). Additionally, we have used AOD at 10 × 10 km to better characterize the trend over urban hotspots. The time-series modelling using ARIMA was used to extrapolate the existing time series for predicting future aerosol loads. Further, non-parametric wind regression (NWR) has been used to apportion the possible source fields of atmospheric aerosols over different stations to assess their transport behavior. Such findings may be crucial in identifying aerosol distribution over IGP, to recognize aerosol characteristics over urban hotspots, mechanism of inter-continental transport, and for forecasting aerosol trend.

2. Data and methods

2.1. Site description

Satellite based aerosol climatology were derived over nine stations across IGP to account the heterogeneity in aerosol micro-physical properties, particle size, emission sources and meteorological conditions. The stations that represent the upper IGP are Karachi, Multan and Lahore (Pakistan); New Delhi, Kanpur, Varanasi and Patna (India) represent the central IGP, and Kolkata (India) and Dhaka (Bangladesh) represent the lower IGP (Fig. 1).

Karachi (24.87°N, 67.03°E) represents a typical urban setting with a variety of air pollution sources including industrial and vehicular emissions, dust storms and sea salts (Khwaja et al., 2009). Multan (30.19°N, 71.47°E) is located in the central part of Punjab province, Pakistan, with vehicular emissions and crustal sources as the major aerosol sources (Alam et al., 2011). A sharp seasonality in the aerosol loading and type has been reported for Lahore (31.54°N, 74.32°E), with vehicular and industrial emissions, biomass burning, transported dusts and fossil fuel combustion-related particles recognized as the principal aerosol sources (Gupta et al., 2013). New Delhi (28.57°N, 77.11°E), the capital city of India, experiences a variety of aerosol sources, with dominance of dust during the pre-monsoon (Pandithurai et al., 2008) while abundance of fine anthropogenic aerosols has been reported during the post-monsoon and winter (Sen et al., 2017). Kanpur (26.45°N, 80.33°E) is characterized by medium to large scale industries along with biomass and refuse burning emissions. Varanasi (25.16°N, 82.59°E) represents an urban location at central IGP, having high aerosol loading from diverse sources like crustal and vehicular emissions, biomass and waste incineration, and from aerosols of transboundary origin (Murari et al., 2016, 2017; Sen et al., 2017). Patna (25.36°N, 85.07°E) is one of the most polluted cities at central IGP with variety of aerosol sources leading to high AOD (Ramachandran et al., 2012). The nature of aerosols over the lower part of IGP is highly influenced by the continental outflow from the upper and central IGP (Singh et al., 2017a; Srinivas and Sarin, 2014). Kolkata (22.33°N, 88.20°E) experiences high aerosol loading during pre-monsoon and winter (Prasad and Singh, 2007), which originates both from continental and marine sources. Dhaka (23.73°N, 90.39°E) is a typical Asian megacity, dominated by fine absorbing aerosols throughout the year, mainly originated from vehicular sources, household energy practices and emissions from brick kilns (Begum et al., 2013; Singh et al., 2017a).

2.2. Dataset and processing

2.2.1. Terra MODIS aerosol optical depth (AOD)

Aerosol optical depth at 550 nm was retrieved on a daily basis from MODIS onboard Terra satellite. MODIS measures spectral radiances from 0.41 to 14 μm (total of 36 wavelengths) with a swath of 2 330 km, and provides near-global daily coverage. MODIS AOD was extracted for every single pixel over entire IGP, and multiyear time series was made by spatial average. AOD was also retrieved over individual stations within a sampling window of 5 × 5 pixels centred over the station. Second generation Collection 6 (C6) level 2 Deep Blue (DB) AOD (Deep_Blue_Aerosol_Optical_Depth_550_Land_Best_Estimate), with the recommended quality flags (QA ≥ 2(2&3)), was used, with data covering 10 years (January 2006 to December 2015). The enhanced DB algorithm was shown to perform better when retrieving aerosol due to improved assessment of NDVI-dependent surface reflectance, cloud screening and better identification of dust (Hsu et al., 2013). It has an additional advantage of extended applicability over arid/desert region as well as over almost any land cover, except ice/snow. Furthermore, the DB algorithm estimates surface reflectance better and has been found to perform better in retrieving aerosol across IGP (Mhawish et al., 2017). The expected error (EE) of the DB over land is ± (0.05 + 20%) (Hsu et al., 2013).

2.2.2. Angstrom exponent (AE)

Angstrom exponent (AE, α) was retrieved at all the nine stations from MODIS C6 level 2 DB AOD. The Angstrom exponent deliver qualitative information regarding aerosol size distribution; hence it was only used for qualitative analysis. The relationship between AOD and AE is used to assess the aerosol loadings and the particle size (Kumar et al., 2015b). Moreover, the dependency of AE on AOD was also investigated and utilized to determine different aerosol types.

2.2.3. Air mass back trajectories

Five-days isentropic air mass back trajectories for individual station were calculated by Hybrid Single Particle Lagrangian Trajectory (HYSPLIT) model (Draxler and Hess, 1998) using GDAS (0.5° × 0.5°) archived data set. HYSPLIT was used for apportioning the potential emission source region for selected stations. Further, concentration weighted trajectories (CWT) were drawn to evaluate variability in potential aerosol source fields that influence the columnar aerosol load at individual stations. The CWT analysis assigns the values of columnar AOD to the respective backward trajectory and allocates the weighted concentration to sequence of grid cells based on the cell specific residence time of the air mass (Gogoi et al., 2014). This can help in quantifying the influence of each advection pathways toward the total observed aerosol load, and estimate a spatial pattern for potential aerosol sources. Mathematically, CWT can be expressed as:

$$CWT_{i,j} = \frac{\sum_{l=1}^{L} C_l . \zeta_{ijl}}{\sum_{l=1}^{L} \zeta_{ijl}} \quad (1)$$

where $CWT_{i,j}$ is the average weighted concentration in a grid cell (i, j), C_l is the measured aerosol concentration (here AOD), ζ_{ijl} is the number of trajectory endpoints in the grid cell (i, j) associated with the C_l sample, and L is the total number of back trajectories over a time period.

Accounting 5-days air mass history was based on the residence time of aerosols, which is of the order of a week in the lower atmosphere (Kumar and Verma, 2016). However, the aerosol chemistry is quite dynamic on a scale much shorter than the aerosol lifeterm, hence put some limitations in apportioning its specific sources. The air mass back trajectories on each day with AOD retrieval for all nine stations were computed at 06:00 h UTC (11:30 h IST; closest to Terra overpass time at 10:30 h) at 500 m, 1 000 m and 2 500 m above ground level. The air masses for different stations were subject to cluster and CWT analysis, and used for delineating their possible source regions. In our previous work for IGP, identical approach has been used considering only near surface particulate mass concentrations (Sen et al., 2017). However, for the present analysis columnar aerosol loading was used to derive potential source fields.

2.3. Statistical analysis and modelling

2.3.1. Mann-Kendall (M-K) test and seasonal Kendall Trend Test (SKTT)

The multi-year trends in AOD over all the stations were estimated using a non-parametric statistical analysis like Mann-Kendall (M-K) test. First proposed by Mann (1945) and further extended by Kendall (1975), the M-K test is used to estimate the monotonic trends in time series data. The M-K test has been applied extensively to estimate aerosol trend globally (Zhao et al., 2017; Maghrabi and Alotaibi, 2017; Li et al., 2014), while its application over Indian sub-continent is limited (Srivastava and Saran, 2017). We applied the M-K test with the null hypothesis (H_0) considering no trend exists in the AOD retrieved over any individual station. The three alternative hypotheses (H_1) were that there is a negative, a non-null, or a positive trend in the data. The M-K test uses Kendall's tau statistic, which is a measure of association between two samples within a time series based on the ranks within the samples (Bennouna et al., 2014). Time series of atmospheric parameters are usually affected by seasonality, which should be addressed when studying long time trends. The seasonal Kendall Trend Test (SKTT) is significantly robust to seasonality and was therefore applied on an annual basis. The “standard” M-K test was used for studying trends within the season. The M-K test is suitable for evaluating long-term trend with non-normal distribution and with missing and/or extreme values. It is however prone to be affected by autocorrelation between the observations and persistence of seasonality within the data. Therefore, the presence of lag-1 autocorrelations was removed and seasonality at all the stations were nullified by pre-whitening of extreme data, followed by the construction of a de-seasonalized AOD time series. The de-seasonalization of monthly averaged AOD time series data was accomplished using seasonal trend decomposition based on Loess (STL) functions.

2.3.2. Time series analysis and autoregressive moving average

Time series analysis is commonly used to understand variations in long-term climatic data, and has been widely used for predicting future trend (Soni et al., 2015). The use of time series analysis is based on the notion that there is some internal structure within the data, e.g. autocorrelation, trends, or seasonal variation. Time series analysis in air pollution studies have been applied using autoregressive, fractal analysis (Yuval and Broday, 2010) and moving average models, and by using a combination of both, known as an autoregressive integrated moving average (ARIMA, Soni et al., 2014; Abish and Mohanakumar, 2013). The ARIMA is an iterative and exploratory process that is applied to best-fit long-term observations. Three steps *viz*. identification, estimation and diagnostic checking ensure the accuracy of time series forecasting. Autocorrelation functions (ACF) and partial autocorrelation functions (PACF) were computed for sequential lags in the data series together with their 95% confidence bounds. We applied ARIMA to predict AOD both for entire IGP as well as for individual stations. It was applied primarily for a short-term forecast of AOD and evaluation of the model suitability for long-term forecasts. Such forecasts are especially helpful in framing appropriate policies for air quality management and other climate related issues.

3. Results and discussion

3.1. Aerosol climatology over IGP

3.1.1. Spatial distribution of aerosols

The area weighted average AOD over IGP reveals a massive aerosol burden (mean ± SD: 0.50 ± 0.25), considerably higher than the global average (0.126), as well as AODs reported over other continents (North America: 0.098; Africa: 0.168; Asia: 0.182; Table 1). Spatial analysis of AOD was further made in two contexts, for the entire IGP considering every single pixel, and for individual stations across IGP. Fig. 2 presents the decadal (2006–2015) variation of average AOD and AE across IGP, indicating a variable pattern in its distribution. The upper IGP is characterized by a low aerosol loading (AOD < 0.45) in comparison to the central and lower IGP, with dominance of coarse aerosols especially over Kharan, Thal and Cholistan Desert region. Interestingly these regions are also associated with comparatively low AOD with prevalence of dust aerosols. It is noteworthy that the central part of Sindh and Punjab provinces in the upper IGP exhibits slightly higher AOD (0.50–0.70) with AE (0.36–1.20) that corresponds to coarse and mixed aerosols. The region indicates the bank of river Indus, which serves as the major food basket of Pakistan, and therefore has huge population load and associated emissions. In comparison to the upper part, both the central and lower IGP are having more consistent distribution of columnar aerosol loading with AOD varying within a range of 0.60–0.70. The most striking feature in Fig. 2 is the persistence of exceptionally high AOD (> 0.80) in the eastern part of the Gangetic plain, mostly within the eastern Uttar Pradesh and north and central Bihar (hereafter referred as the aerosol pool). Previously designated ‘the Bihar pollution pool” (Di Girolamo et al., 2004), the aerosol pool poses the similar characteristics like Indus valley of Pakistan, having varying aerosol sources mainly from fossil fuel consumption (Singh et al., 2017a), biofuels used for household cooking, and burning of agricultural residues and waste material (Banerjee et al., 2015, 2017). Another unique feature appeared in Fig. 2 is regionality in aerosol type,

Table 1
Decadal mean of aerosol optical depth over different geographical regions.

Region	Mean AOD	Period of study	Data source	References
Indo-Gangetic Plain	0.503	2006–15	MOD04*	Present study
Middle East	0.010–0.030	2000–15	MOD04	Klingmüller et al., 2016
Iberian Peninsula	0.130	2000–09	MOD04	Granadoz-Munoz et al., 2011
Asia	0.182	2003–12	MOD04 and MYD04	Mao et al., 2014
Europe	0.099	2003–12	MOD04 and MYD04	Mao et al., 2014
Africa	0.168	2003–12	MOD04 and MYD04	Mao et al., 2014
North America	0.098	2003–12	MOD04 and MYD04	Mao et al., 2014
South America	0.119	2003–12	MOD04 and MYD04	Mao et al., 2014
Global	0.126	2003–12	MOD04 and MYD04	Mao et al., 2014

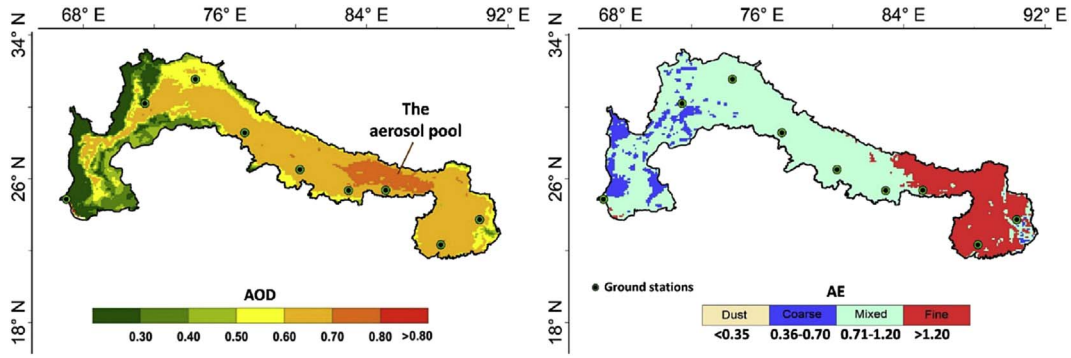

Fig. 2. Decadal (2006–2015) variation of averaged AOD and AE across IGP.

with dominance of mixed aerosols over central IGP while fine aerosols consistently dominated on the lower part. Although the particulate emission characteristics throughout the IGP are very similar (Singh et al., 2017a), the persistence of fine aerosols over the lower IGP is mainly associated to local meteorology and topographical factors. The variability of aerosol types mainly attributed to seasonal variations in particulate source strength and meteorology (Mhawish et al., 2017). Alam et al. (2011) also highlighted the seasonal basis of distinct aerosol transport, which leads to an accumulation of different types of aerosols over the region. Indeed, Sen et al. (2016, 2017) and Kumar et al. (2015b) recognized the transport of coarse airborne particles from western dry regions (upper IGP) to the central and lower IGP by means of the prevailing westerlies. These coarse particulates eventually settle over the subsidence zone (Di Girolamo et al., 2004) that overlaps the aerosol pool and adjoining regions in central and lower IGP, leading to an enhanced concentration of mixed aerosols. However, relative contribution of transboundary coarse particulates gradually diminishes towards the lower part of IGP, therefore, despite having almost similar source characteristics, lower IGP results to a dominance of fine aerosols.

The AOD over individual stations are in line with the general spatial pattern (Fig. 3). Stations in the upper IGP (decadal mean ± SD; Karachi: 0.34 ± 0.47; Multan: 0.27 ± 0.11; Lahore: 0.50 ± 0.15) experienced minimum columnar aerosol loading in comparison to the stations in central and lower part (Table 2). However, such low AOD retrievals over the upper IGP are in contrast to AOD as reported by Alam et al. (2011) for Pakistan. Such discrepancy may be due to the selection of MODIS C5 Dark Target (DT) algorithm, which overestimated the AOD due to uncertainty in its surface reflectance estimates over brighter surfaces (Bilal et al., 2016). In contrast to the upper IGP, comparatively higher AOD is evident over the central IGP: Delhi (0.58 ± 0.22), Kanpur (0.63 ± 0.24), Varanasi (0.67 ± 0.28) and Patna (0.65 ± 0.30). The additive increment of aerosol load from the upper to the lower regions of the central IGP highlights pollution transport in the downwind, resulting in a sustained rise of long-term AOD (Kaskaoutis et al., 2012). Aerosol loading over the lower IGP (Kolkata: 0.58 ± 0.21; Dhaka: 0.60 ± 0.24) is virtually similar to the AOD in the central IGP (Fig. 3), but with an overall dominance of fine aerosols (Fig. 2).

Fig. 4 reports the magnitude of the inter-annual variability in AOD (standard deviation of mean), ranging between 31% (Lahore) and 47% (Patna). The differences in magnitudes of inter-annual AOD variations especially correspond to the diverse aerosol sources that exists across entire IGP, having an overall inter-annual variability of 31.4%. The regional features of anomalous aerosol variation over the years emphasize different degrees of inhomogeneity in the aerosol loading. Comparatively higher rate of increase in AOD was evident particularly over stations that are located within the aerosol pool (Varanasi and Patna). Subsidence of north-westerly wind over these regions inhibits vertical mixing of airborne particulates and thereby, facilitates gradual accumulation of aerosols (Dey and Di Girolamo, 2011; Kumar et al., 2015b, 2017a). Although the entire IGP experiences such subsidence, the region with highest subsidence extends from central to lower IGP, especially over the aerosol pool region, which characteristically shows significant increase in AOD.

3.1.2. Temporal distribution of aerosols

Temporal variation in aerosols across the IGP is mainly associated with seasonality, which is related to both the intensities of natural sources and anthropogenic emissions. In particular, seasonal variations in aerosol properties is related to local agriculture practices, livelihood and meteorology. Keeping in view of such seasonal variations, aerosol climatology was derived for different seasons like pre-monsoon (MAM), monsoon (JJAS), post-monsoon (ON) and winter (DJF). Variation of the AOD and AE (Fig. 5a–b) at different seasons show distinct regional patterns during pre-monsoon, with relatively low AOD (0.45 ± 0.10) and dominance of coarse particles (AE: 0.72 ± 0.30). Sources of pre-monsoon aerosols over IGP are resuspended dust, mainly from agricultural fields and unpaved roads, yet transported dust from Thar and West Asian dry regions also contribute substantially to the regional aerosols (Giles et al., 2011; Singh et al., 2017a). Additionally, strong convective winds further facilitate vertical advection of aerosols, even up to the Himalayas, thereby increasing its residence time. Both observational (Gautam et al., 2011) and model (Henriksson et al., 2011) studies suggest that the mineral dust induce major contribution to total AOD during pre-monsoon while fine particulates are dominant during rest of the year. The entire IGP exhibits almost uniform moderate

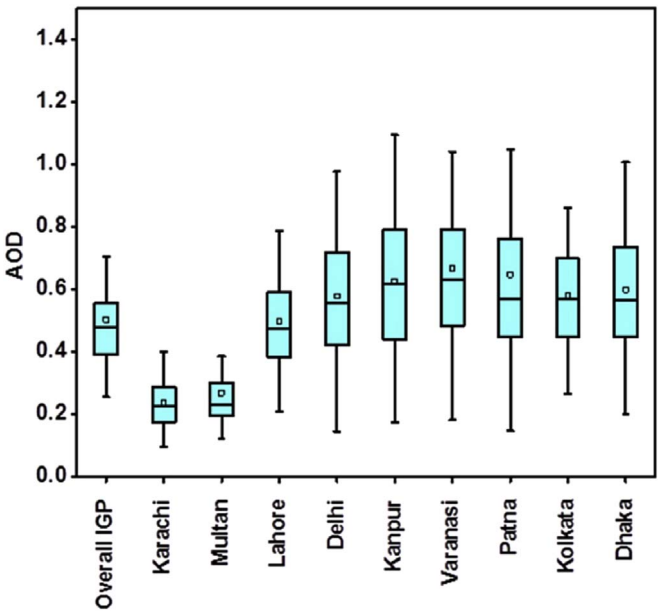

Fig. 3. Decadal variation of AOD over IGP and for individual stations across IGP.

Table 2
Descriptive statistics of aerosol optical depths over different stations across IGP.

Statistics	IGP	Karachi	Multan	Lahore	Delhi	Kanpur	Varanasi	Patna	Kolkata	Dhaka
Minimum	0.26	0.10	0.12	0.21	0.15	0.08	0.09	0.08	0.07	0.15
Maximum	1.13	3.50	0.80	0.92	1.32	1.27	1.54	1.95	1.42	1.53
1st Quartile	0.39	0.19	0.20	0.39	0.42	0.44	0.49	0.45	0.45	0.45
Median	0.48	0.24	0.23	0.47	0.56	0.62	0.63	0.57	0.57	0.56
3rd Quartile	0.55	0.30	0.30	0.58	0.72	0.79	0.79	0.76	0.70	0.72
Mean	0.50	0.34	0.27	0.50	0.58	0.63	0.67	0.65	0.58	0.60
Variance	0.03	0.22	0.01	0.02	0.05	0.06	0.08	0.09	0.04	0.06
Std. Dev.	0.16	0.47	0.11	0.15	0.22	0.24	0.28	0.30	0.21	0.24
Coeff of Var.	0.31	1.36	0.42	0.31	0.38	0.39	0.42	0.47	0.35	0.39
Skewness	1.42	5.34	1.91	0.59	0.50	0.42	0.69	1.45	0.84	0.83
Standard error	0.01	0.04	0.01	0.01	0.02	0.02	0.03	0.03	0.02	0.02
Geometric mean	0.48	0.26	0.25	0.48	0.53	0.58	0.60	0.58	0.54	0.55
Inter-annual variability (%)	31.4	34.3	42.7	30.7	38.4	38.5	42.3	47.1	35.3	39.0

aerosol loading (0.4–0.8) during pre-monsoon, with few patches of low AODs (< 0.4) particularly over Baluchistan (in upper IGP). Identical pattern is also observed at the individual stations. For example, stations over upper IGP exhibit comparatively lower AOD (Karachi: 0.27; Lahore: 0.40; Multan: 0.24), whereas at the other stations moderate AOD were noted, and remain within 0.47 (Delhi) to 0.64 (Dhaka). In contrast, variation in the aerosol size distribution are evident, with dominance of coarser particles at upper IGP and in few parts of central IGP, while finer aerosols mostly prevail over central to lower IGP. A distinct aerosol size distribution characteristic is evident over central IGP, with dominance of mixed aerosols over the north sections, and coarser aerosols over regions located in the southern part. Dominance of fine particulates in pre-monsoon is only observed over the lower IGP, with high AE (Kolkata: 1.39; Dhaka: 1.06) as household energy practices, small scale industries, biomass and waste burning considerably contribute to the generation of fine aerosols (Karar and Gupta, 2007).

The columnar aerosol loading comparatively enhanced during monsoon (AOD, mean ± SD: 0.54 ± 0.17), most notably over the upper IGP (Karachi: 0.58, Multan: 0.33; Lahore: 0.47). Karachi being the closest to the Arabian sea is reported to be affected by south westerly wind during monsoon, which carries sea salt aerosols, resulting increase in AOD (Bilal et al., 2016). The exponential increase in AOD in highly humid condition (RH > 85%) is mostly attributed to the hygroscopic growth of fine particulates (Altaratz et al., 2013). However, increase in AOD due to hygroscopic growth of particles is more prominent near sea coast (like in Karachi), possibly due to the immediate effect of available moisture which increase the extinction coefficient. However, as the moisture laden bulkier particles drift away from the coast to inner continental regions (like Multan to Lahore), their deposition increases, resulting in a gradual reduction in AOD. This explains the varying effects of particle hygroscopicity on overall columnar aerosol loading and were in accordance to Kaufman et al. (2005). The increasing trend is more notable over upper IGP, like in Karachi (0.57), Lahore (0.47) and Multan (0.33), while AOD over Patna (0.52) and Kolkata (0.56) also show an increase compared to pre-monsoon. Yet, while the general trend is increasing, few stations in central (Varanasi: 0.49; Patna: 0.52; Kanpur: 0.54) and lower IGP (Dhaka: 0.50) reveal a comparable or marginally reduced AOD during monsoon, possibly

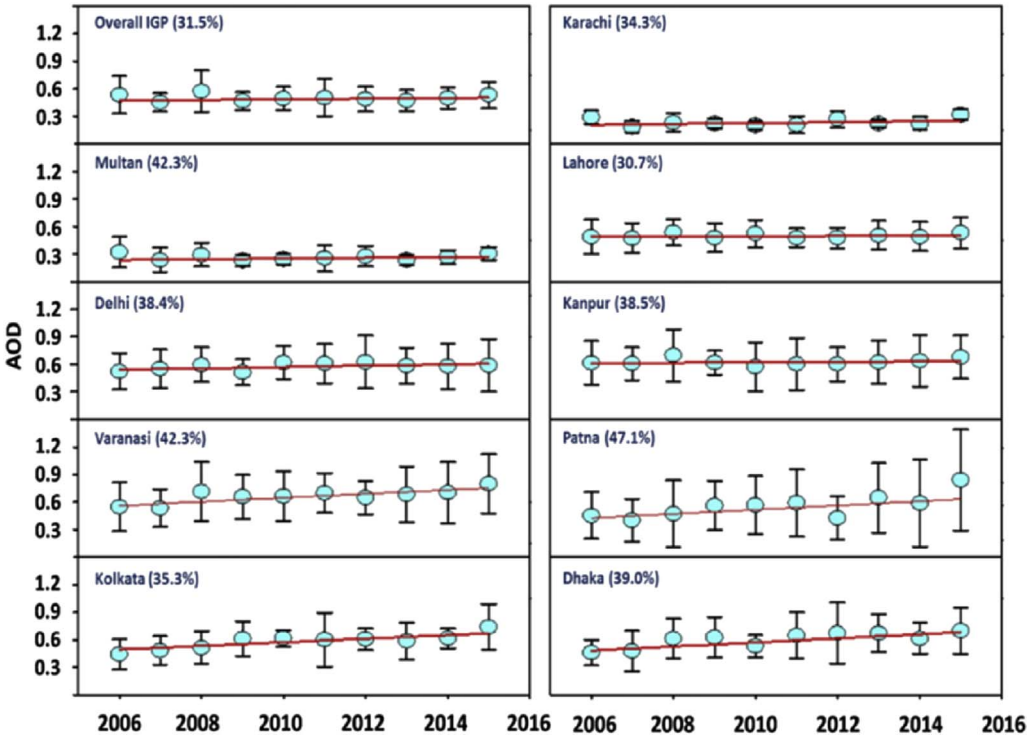

Fig. 4. Inter-annual variation, linear trend (red line) and inter-annual variability of AOD (within parenthesis) for individual stations across IGP. (For interpretation of the references to color in this figure legend, the reader is referred to the Web version of this article.)

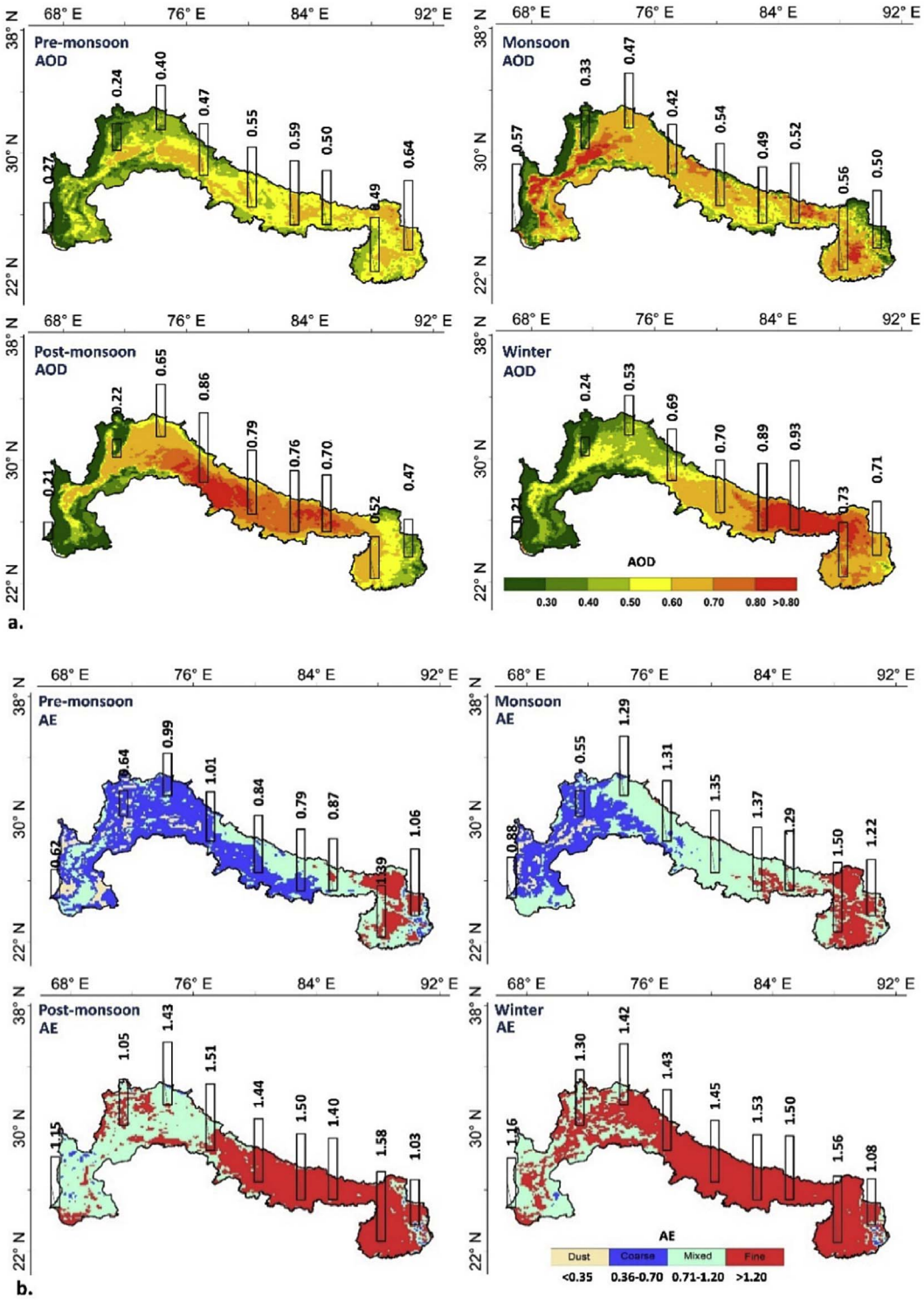

Fig. 5. Spatial distribution of seasonal mean (a) AOD and (b) AE for 2006–2015 over IGP.

influenced by wet removal of particles. This indicates the change in AOD over IGP is not always associated with particular urban centre but translates across the region. Variation of aerosol size follows this existing trend, with dust and coarser aerosols dominating over the upper IGP, and predominately mixed type aerosols over the central IGP. Decadal average of AE at individual station differs however from the regional trend, possibly due to influence of local emissions, with Karachi (AE: 0.88) and Multan (AE: 0.56) revealing dominance of coarser particulates, while all the remaining stations exhibit prevalence of fine particles (AE: 1.2 to 1.5).

Spatial distribution of columnar aerosol loading both in terms of AOD and AE are almost similar for winter and post-monsoon. Both seasons exhibit similar aerosol source profiles, mainly dominated by biomass/waste burning and vehicular emissions (Banerjee et al., 2015; Singh et al., 2017a). However, agricultural residue burning mostly govern aerosol climatology during post-monsoon, while winter is mainly associated to shallow boundary layer, and emissions from burning of both biomass and waste (Kumar et al., 2015b, 2017a). The

area weighted mean AOD for the entire IGP remain comparable for post-monsoon (0.55 ± 0.20) and winter (0.52 ± 0.20), in identical to AE (post-monsoon: 1.19 ± 0.21; winter: 1.31 ± 0.19). Across IGP, aerosol loadings during post-monsoon and winter have two characteristic signatures. First, upper IGP continues to have low columnar aerosol profile with overall dominance of mixed type of aerosols during post-monsoon, with greater accumulation of fine particulates during winter. All three stations over upper IGP exhibit similar kind of pattern with minor increase in AE from post-monsoon (AE: 1.1–1.4) to winter (AE: 1.2–1.5). Second, fine particulates completely engulfed the central to lower IGP, and the relatively higher AOD (> 0.80) that exists over central IGP during post-monsoon appears to move downwind during winter. Such phenomenon may be explained considering post-monsoon specific crop residue burning over upper IGP, which leads to increase in AOD over Lahore (0.65), Delhi (0.86) and Kanpur (0.79), before being transported towards lower IGP in winter by prevailing northwesterly, and contribute to AOD in Varanasi (0.89), Patna (0.93), Kolkata (0.73) and Dhaka (0.71). Such aerosol climatology, facilitated by regional topography and synoptic scale meteorology, poses greater uncertainty in recognizing aerosol-induced change in regional air quality and climate change.

3.2. Aerosol loading trend over IGP

The monotonic trend in AOD for the entire IGP and over different stations across IGP was assessed using the non-parametric Mann-

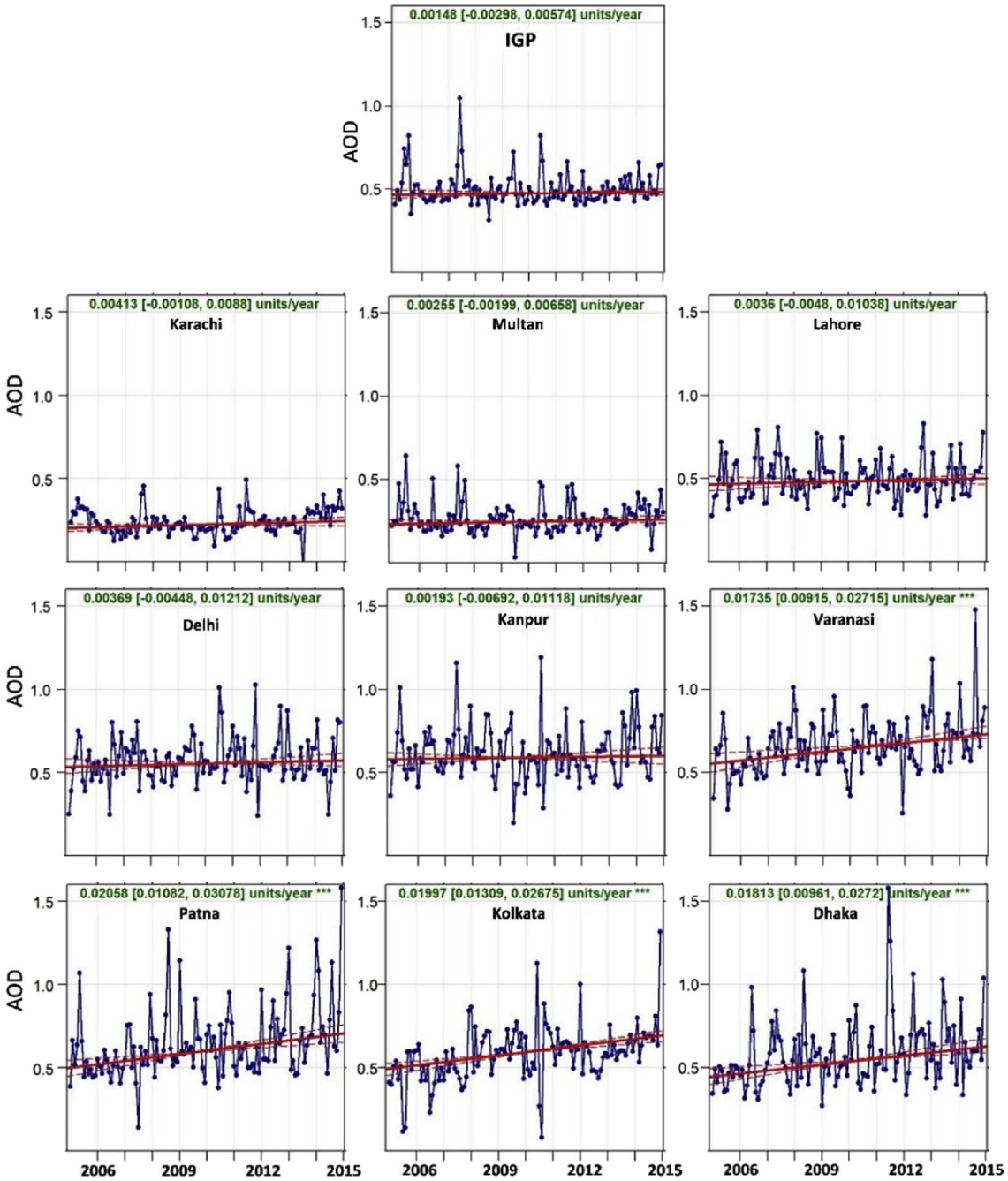

Fig. 6. Comparison of decadal trends in AOD for entire IGP and for all stations across IGP. Note: The plot shows the decadal trends in AOD over different locations of IGP. Blue line signifies the monthly averaged AOD time series. The solid red line shows the trend estimate and the dashed red lines show the 95% confidence intervals for the trend based on resampling methods. The overall trend is shown with green color as unit per year, and the values inside the parenthesis denote the 95% confidence interval limits. (For interpretation of the references to color in this figure legend, the reader is referred to the Web version of this article.)

Kendall test. Here we have presented both spatial and seasonal pattern of the trend, measured in terms of changes in AOD, and further quantified for each urban hotspot.

3.2.1. Decadal trend analysis

The long-term aerosol climatology, namely non-parametric monotonic changes in de-seasonalized AOD time series for the entire IGP and for individual stations is presented in Fig. 6. The annual rate of change in AOD and the Theil Sen's slope, indicating the overall change in trend (positive or negative), are also shown. A statistically insignificant increasing trend of 0.002 year^{-1} is computed for the entire region. Considering the massive population, urban development and anthropogenic emissions, the decadal trend in AOD is rather low. This may possibly indicate that the spatial variation in columnar AOD is more affected by seasonality and topography of the region, and primarily concentrated over few urban hotspots. The trend is comparable to that of 0.005 year^{-1} as reported by Streets et al. (2009) using chemical transport model coupled with emissions inventory for entire India (1980–2006). Our estimated trend is also comparable to the trend (0.007 year^{-1}) reported by Krishna Moorthy et al. (2013) over northern India (2001–2011) using AOD from Multiwavelength spectroradiometer, but considerably lower than that of 0.01–0.04 year^{-1}, as reported by Dey and Di Girolamo (2011) for the IGP using AOD retrieved from MISR (2000–2010). Differences in aerosol loading trends by different researchers are attributed to differences in the period of observation, resolution and data frequency, and type of statistical analysis performed (parametric or non-parametric; neighborhood information). Yet, they may also suggest high sensitivity of the multi-annual AOD trend to ordinary least-square method (OLS), which may occur when the year-to-year variation is much larger than the mean (low SNR). Alternatively, autocorrelation in the residuals (after accounting for seasonality in the time-series) may also affect the slope (and statistical significance tests, such as M-K).

To our knowledge, this analysis is the first comprehensive attempt to recognize spatial and temporal changes in aerosol climatology over IGP considering enhanced 'second generation' MODIS C6 DB AOD data. Consideration of enhanced MODIS DB algorithm was helpful for improved estimation of AOD, as DB was able to retrieve AOD over 10732 pixels (covering 99.7% of total geographical area), especially over bright arid/desert regions of upper IGP, with better estimation of surface reflectance. However, our analysis was not able to classify the observed trend to specific regions within the IGP and recognize pollution hotpot. Instead, we considered few important urban stations, well distributed across the geographical region to recognize local trend. Considering the inter and intra-seasonal variability in AOD across IGP, decadal trends were computed for two scenarios: with de-

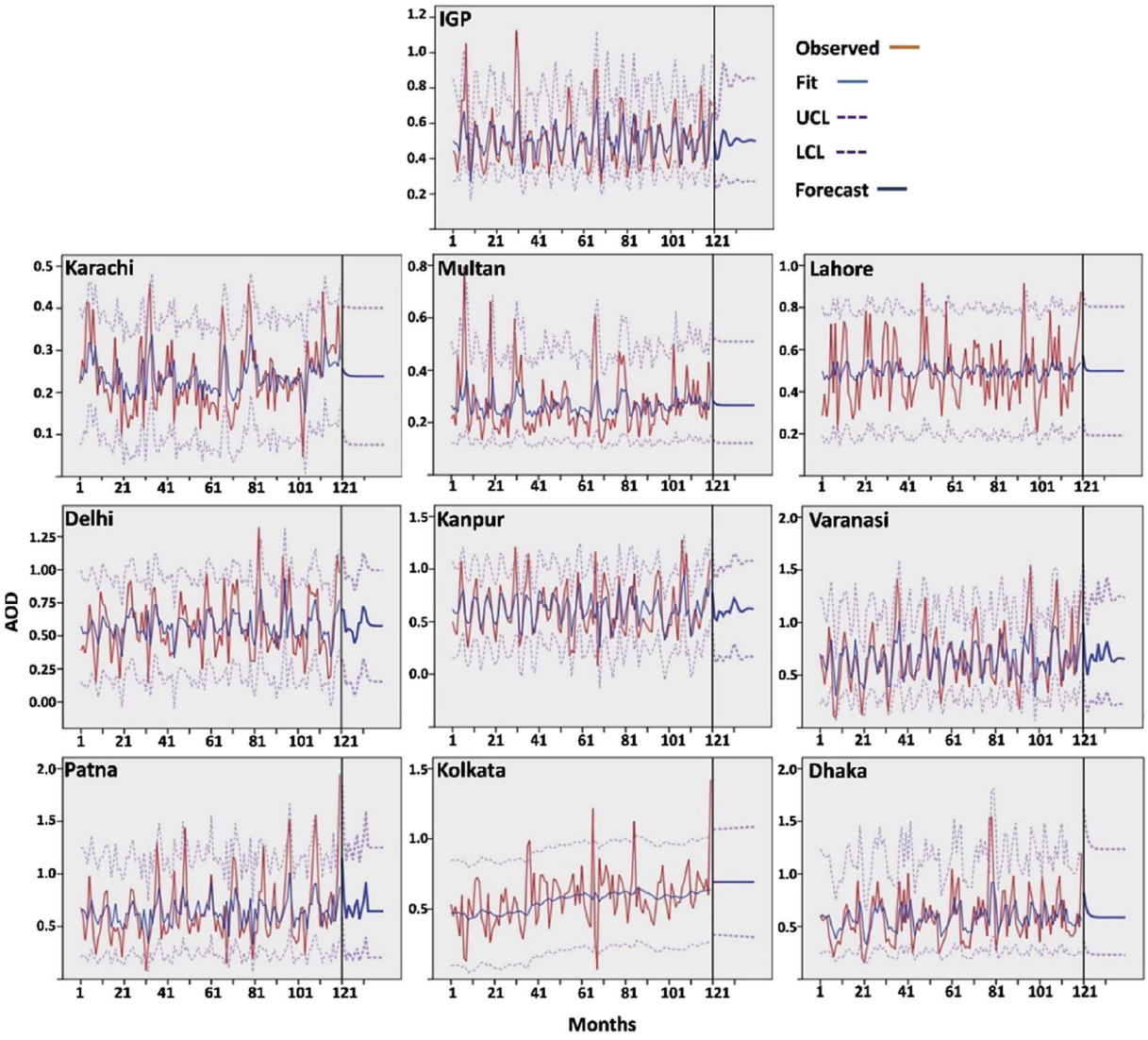

Fig. 7. Comparison of ARIMA model simulations (blue line) with MODIS AOD (red line) and forecasting of AOD across IGP. (For interpretation of the references to color in this figure legend, the reader is referred to the Web version of this article.)

seasonalization of the monthly mean AOD time series, and by analyzing season-specific trends at individual stations without de-seasonalization. Considering the entire time series AOD, we achieved two specific findings: all incurred stations across IGP revealed a positive trend (either significant or not) with nonetheless spatial variation, and stations in central and lower-IGP appear to have comparatively higher and statistically significant trend. Across IGP, trend values vary from 0.0019 (Kanpur) to 0.0206 year^{-1} (Patna), while for stations located at upper IGP and in the northern part of central IGP appeared to have comparatively lower and non-significant increasing AOD trend. In contrast, all the four stations from central to lower IGP i.e. Varanasi (0.0174 year^{-1}), Patna (0.0206 year^{-1}) Kolkata (0.0200 year^{-1}) and Dhaka (0.0181 year^{-1}), depict almost identical trend with high magnitude of Theil Sen's slope (0.012–0.019), confirming the validity of the increasing trend.

Sectoral emissions of air pollution, reflected by various literature indicate residential/agricultural biomass burning, vehicular and industrial growth, demand for energy as principal sources of aerosols over IGP (Reddy and Venkataraman, 2002; Saud et al., 2011; Singh et al., 2017a,b). An estimated rise in the industry (I), transport (T), agriculture (A) and residential (R) emissions of $PM_{2.5}$ (I,T: 30%; A,R: 14%), BC (I,T: 21.7%; A,R: 27%) and other aerosol precursors i.e. NOx (I,T: 45.4%; A,R: 35%) and SO_2 (I,T: 51.0%; A,R: 36%; Sadavarte and Venkataraman, 2014; Pandey et al., 2014) from 2005 to 2015 are consistent with the rise in columnar aerosol load. Also, emission estimates from Green House-Air Pollution Interactions and Synergies (GAINS) based model revealed a 7.6% growth in the BC emissions in India from 2005 to 2015, and is further projected to increase by 19.2% till 2030. The population growth over IGP, especially over urban centres, with enhanced residential biomass/waste burning is closely linked with increasing AOD. The central IGP stations, falling within Bihar (Patna) and Uttar Pradesh (Varanasi and Kanpur) were reported to have significant contribution (as high as 17–21%) from residential biomass burning (Saud et al., 2011). Recent satellite measurements have also revealed that India has overtaken China to become largest emitter of SO_2 with 50% increased emissions (Li et al., 2017), endorsing the escalated emission estimates. Not limited to this, IGP represents one of the highly fertile regions of the world, having intensive agricultural practices using high dosages of nitrogen based fertilizer. A recent rise in the use of these fertilizer (3.6%, Warner et al., 2017) induce generation of ammonia, and thereby aerosol particles through gas-to-particle conversion (Sharma et al., 2014, 2017). The sectoral emission scenarios over stations located in Pakistan typically represents IGP with majority of aerosol emissions from residential, industrial and transport sectors (Shahid et al., 2015; Singh et al., 2017a). Inadequate information on emission inventories over Pakistan and Bangladesh though limit the analysis, the sharp rise in population, vehicular density and industries in Pakistan and in Bangladesh (Shohel et al., 2017) is potentially associated with increase in aerosol loadings over the decade. However, it should be noted that region with observed change in AOD was not always coincide with urban centres possibly because of additional influence of local meteorology and topographical factors.

3.2.2. Seasonal trend analysis

The distinct pattern of observed trends in AOD over different stations prompted us to analyze the long-term trend on a temporal basis. With the exception of upper IGP stations, all stations were found to show increasing trend in AOD during post-monsoon (Table S1). During winter, the central IGP station adjacent to lower IGP (i.e. Patna) and both stations at lower IGP (Kolkata and Dhaka) also exhibited increasing trends. The overall trend in AOD during pre-monsoon was negative with very few exceptions. The assessment of aerosol trends on temporal basis highlights the insufficient evidence of aerosol contributions of monsoonal and pre-monsoonal AOD, while notable contributions of post-monsoonal and wintertime aerosol to its overall increasing trend. Our observation was in accordance to Pandey et al. (2017), which also reported a significant decline (10–20%) in pre-monsoon aerosol loading over India, even with overall annual increasing trend. Seasonal trend analyses clearly emphasize the post-monsoon and winter as crucial period in terms of aerosol loading, and hence anthropogenic activities during this seasons must be addressed while making any pollution control strategy over the plain.

3.3. Time series modelling and prediction

The Auto Regressive Integrated Moving Average (ARIMA) model was applied for predicting AOD both for the entire IGP, considering area weighted mean, and for the nine stations across the IGP (Fig. 7). The predicted AOD is based on the observed monthly mean AOD between 2006 and 2015, and AOD is forecasted for next 20 months. The model performances are evaluated using various statistical measures, including stationary R^2, normalized root mean square error (NRMSE), mean absolute error (MAE), normal Bayesian information criterion (BIC) and Ljung- Box. Table S2 enlists various model fit statistics of the time series representing the performance of prediction model. The variations in observed and predicted AOD time series that fall between the lower (LCL) and upper (UCL) confidence limits are within the 95% confidence interval, and forecasting within this interlude is considered reliable. The observed and predicted AOD for each station and for the entire IGP are within the UCL and LCL (Table S3), indicating a satisfactory agreement between MODIS and ARIMA based predictions.

At most of the stations, ARIMA predictions follow a combination of trend and random walk (a Brownian time series). The stationary-R^2 is used to evaluate the observed and predicted AODs in a non-stationary time series, which depicts moderate fit between observed and predicted AODs when IGP considered as a whole (stationary-R^2: 0.41), and low to moderate fit at individual stations (0.03–0.42). ARIMA performed better over Karachi (0.21) compared to other upper IGP stations (Multan: 0.13; Lahore: 0.03). The performance of ARIMA improves over central IGP, especially over Kanpur (0.36) and Varanasi (0.42), elucidating better suitability of the model. The ARIMA-based AOD forecast was also found better compared to baseline models, as evident from the low NRMSE (< 0.40). Further, the spatial variability of the stationary-R^2 between the observed and predicted AODs suggest non-robust predictability of the AOD. The R^2 values, another means of evaluation of time series forecast, exhibited some degree of spatial variation. The similarity between the stationary-R^2 and the R^2 indicates that the model is better than the baseline model, and can be effectively used for forecasting aerosol loading. The low NRMSE between observed and predicted AODs over all the stations (< 0.40), and for the entire IGP (0.24) also indicates a reasonable model performance. A reasonable degree of representativeness of the data is observed, based on the negative values of the normalized BIC, which provides a measure for the overall fit of the predicted time series. The normalized BIC reveals a trend similar to that of the NRMSE, with lower values over the upper IGP stations (-5.1 to -3.6) and higher values at central IGP (-3.1 to -2.6). The Ljung– Box model statistic, a diagnostic tool used to indicate the lack of fit of a time series model while accounting for autocorrelation in the residuals, lies between 22.9 and 36.2, with 0.002–0.069 significance level, indicating random distribution of the residuals. The ARIMA based predictions for next 20 months were also validated with MODIS observation (January 2016–August 2017), and agreeable association (r: 0.34–0.66) were noted within most of the stations (not shown).

Based on the collective evaluation of the model output, ARIMA was found to predict reliable AOD across IGP. However, non-stationary behavior of aerosol loading and heterogeneity in the aerosol optical properties induce limitations in the model, which performed rather poorly in Lahore, Kolkata, Karachi and Multan. Previous attempts for forecasting AOD by ARIMA over different stations used either satellite observations or ground-based AOD retrievals. Soni et al. (2014) used AERONET retrieved AOD over central IGP and the Himalayan region,

and MODIS C5 to retrieve AOD over coal fields in eastern (Jharia, Bokaro), central (Korba) and western (Wardha) India (Soni et al., 2015). Satisfactory model performance was found, especially for low AOD conditions (sites) like in Himalayan region. In contrast, over IGP where AOD were comparatively high, the model performance was relatively poor. The spatio-temporal variability in aerosol mass loadings, attributed to a wide variety of sources and associated uncertainties in the MODIS retrieval algorithms (Gupta et al., 2013), resulted in spatial inconsistencies in the observed and predicted AOD. To overcome the effects of non-stationary AOD behavior, more advanced models like adaptive neuro-fuzzy inference system and artificial neural network may be useful.

3.4. Aerosol potential sources fields

To examine the spatial pattern of aerosol sources, CWT analysis was carried out for individual stations across IGP. CWT was used both for annual and for seasonal exploration of the nine stations across IGP, accounting for three heights (500 m, 1 000 m and 2 500 m) on 06:00 h UTC, considering ten years average AOD.

3.4.1. Annual mean CWT analysis

Fig. 8 depicts the CWT source fields for the nine IGP receptor sites. Although the potential sources are mainly located at the W, SW and NW of the respective ground stations, some variations of the source regions are noted. The CWT indicates that the wind blows predominately from the western dry regions, e.g. Pakistan, Afghanistan, western Indian desert regulates the columnar aerosol loading over stations located at upper and central IGP. In contrast, receptor sites in the lower IGP are influenced both by continental aerosols from upper and central IGP, and by marine aerosols from the Bay of Bengal. In the upper IGP, contributions to higher columnar AOD are attributed to cluster trajectories from relatively closer regions. Likewise, moderate aerosol loading at Lahore are mainly originated from nearby areas (CWT: 0.50–0.60), yet aerosols from the western dry regions of Sulaiman range and Thal desert also contribute to the columnar aerosol loading over the city. Western and north western distant regions also feebly contribute to the aerosol masses at Multan.

Delhi is most likely influenced by source fields of local origin, with moderate to high contributions from adjoining north western dry regions, and with occasional contribution from the eastern side of Gangetic plain. High CWT values (0.60–1.00) adjacent to Delhi mainly attributed to continuous local emissions from traffic and industrial activities, often associated with emissions from burning of agro-residues and municipal waste (Sen et al., 2017; Banerjee et al., 2017). Almost identical source fields are noted for the other stations in central IGP, with very high CWT values (0.60–1.00) confined to the north-western upper and central Gangetic stretch, indicating the role of both local and regional sources. In addition, many trajectories that originated at the far north-west semi-arid desert, the central highlands and from the lower Gangetic plains are also evident, particularly at central IGP, indicating diverse regional contributions of aerosol sources to columnar AOD. The high CWT (> 0.60) between Delhi, Varanasi, and Patna indicates the transport route of airborne particles. The contributions of diverse aerosol sources at central IGP results in mixing of locally emitted aerosols and transported aerosols, making their properties heterogeneous and complicated (Kumar et al., 2016, 2017a; Sen et al., 2016, 2017). Over lower IGP, the key source fields that contribute to the aerosol mass are mostly confined to adjacent north-western regions, along with local emission. The marine aerosols are also found to contribute, however, contributions from relatively distant sources (CWT: 0.40–0.50) are much lower. Overall, in addition to local sources, advection from north-western dry part was identified as a principal contributor to the aerosol columnar loading in most of the stations. Nonetheless, when the entire geographical area experiences a strong reversal of wind, namely southwest and the northeast monsoon, the seasonal deviations of the wind field result in prominent change in the aerosol source fields. Owing to the season specific reversibility of wind profile, it seems further essential to understand the seasonal source profile of aerosols for each selected station.

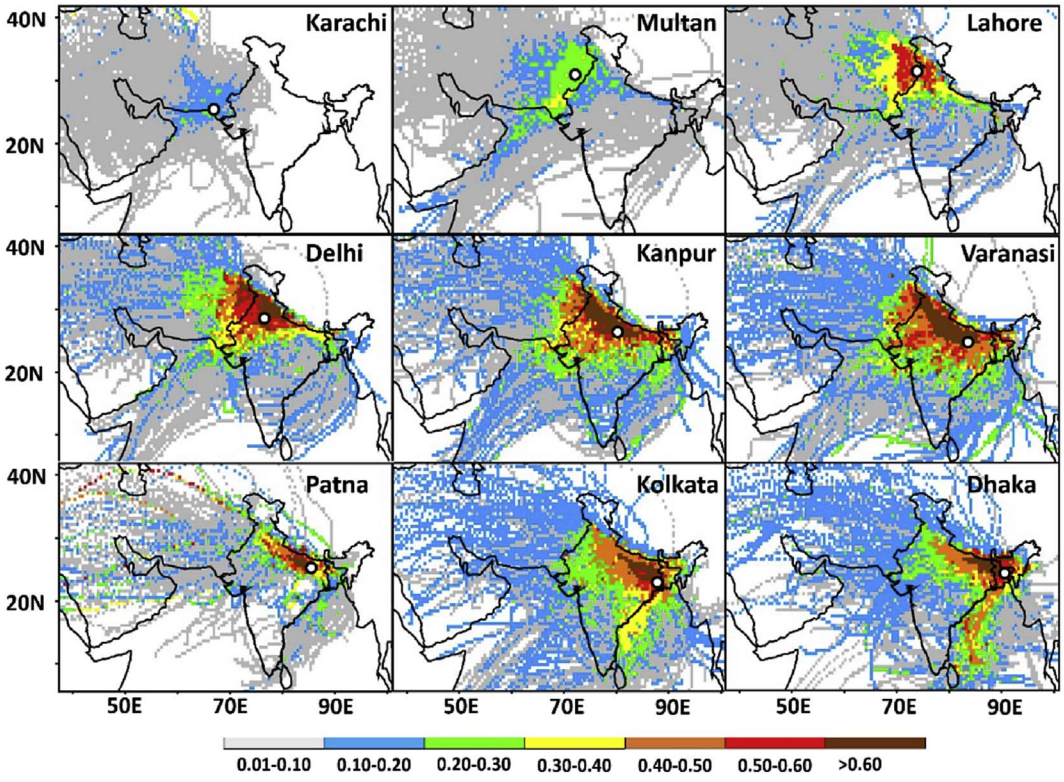

Fig. 8. The annual CWT map for AOD at all stations across IGP during 2006–2015.

3.4.2. Seasonal CWT analysis

Fig. 9 presents the potential aerosol source fields in each season for the nine individual stations. Seasonal mean CWT fields revealed large influence (CWT > 0.50) of potential sources from the upper IGP during winter, moderate influence (CWT > 0.50) from central IGP during post-monsoon, medium (CWT < 0.40) from the upper and central IGP during pre-monsoon, and low source influence (CWT < 0.15) from local areas during monsoon seasons. For stations located at upper IGP, medium to low aerosol source fields (CWT: 0.10–0.40) are evident over western side of the respective stations during pre-monsoon, while very low CWT (< 0.10) are only recognized in the far-west. This emphasizes the contribution of dust and coarse airborne particles, typically from the Arabian or Persian Gulf of Middle-East Asia and from the Kharan, Thal and Cholistan Deserts, to columnar aerosol loading over the upper IGP. Compared to that, stations in central IGP are less prone to pre-monsoon specific dust events. The low intensity source fields (CWT: 0.25–0.40) across the northern belts of IGP are mainly attributed to soil or mineral dusts. The potential aerosol source fields for stations in the lower IGP are predominately oceanic, with additional contributions from the upper Gangetic plain, central highlands and the western dry regions. During monsoon, most of the stations experience aerosols predominately of local origin, as transboundary movement of the aerosols is reduced due to the influence of monsoonal rain.

Extremely high CWT is noted near Lahore, Delhi and adjoining regions of the upper IGP during post-monsoon, which reflects the localized origin of aerosol sources. At the same time, the post-monsoon mean CWT for the central IGP stations depicts similar features (CWT: 0.6–1.0), but highest mean CWT appear to be only from proximate areas. Both upwind and downwind regions showed moderately high CWT (0.5–0.6), which signifies the role of dispersion. Lower IGP stations are less likely to be affected by upwind emission sources and the aerosol loading is mostly contributed by local emissions.

During winter, the upper IGP stations experience high influence of potential source regions from local areas, followed by moderate to medium influences of adjoining regions in the upper IGP. For stations located at central IGP, CWT suggests high potential source fields (0.6–1.0) that are mainly distributed in close proximity to the stations, especially for Delhi and Kanpur. In contrast, Varanasi and Patna experience source contributions (CWT: 0.4–1.0) from the western part of the Gangetic plain. The stations at the lower IGP were also found to be influenced by continental aerosols that mainly originated from the central IGP and from local emission sources. Dhaka was found to be additionally subject to biomass burning emissions from North-Eastern India.

4. Conclusions

The multiyear assessment of MODIS C6 enhanced DB algorithm-

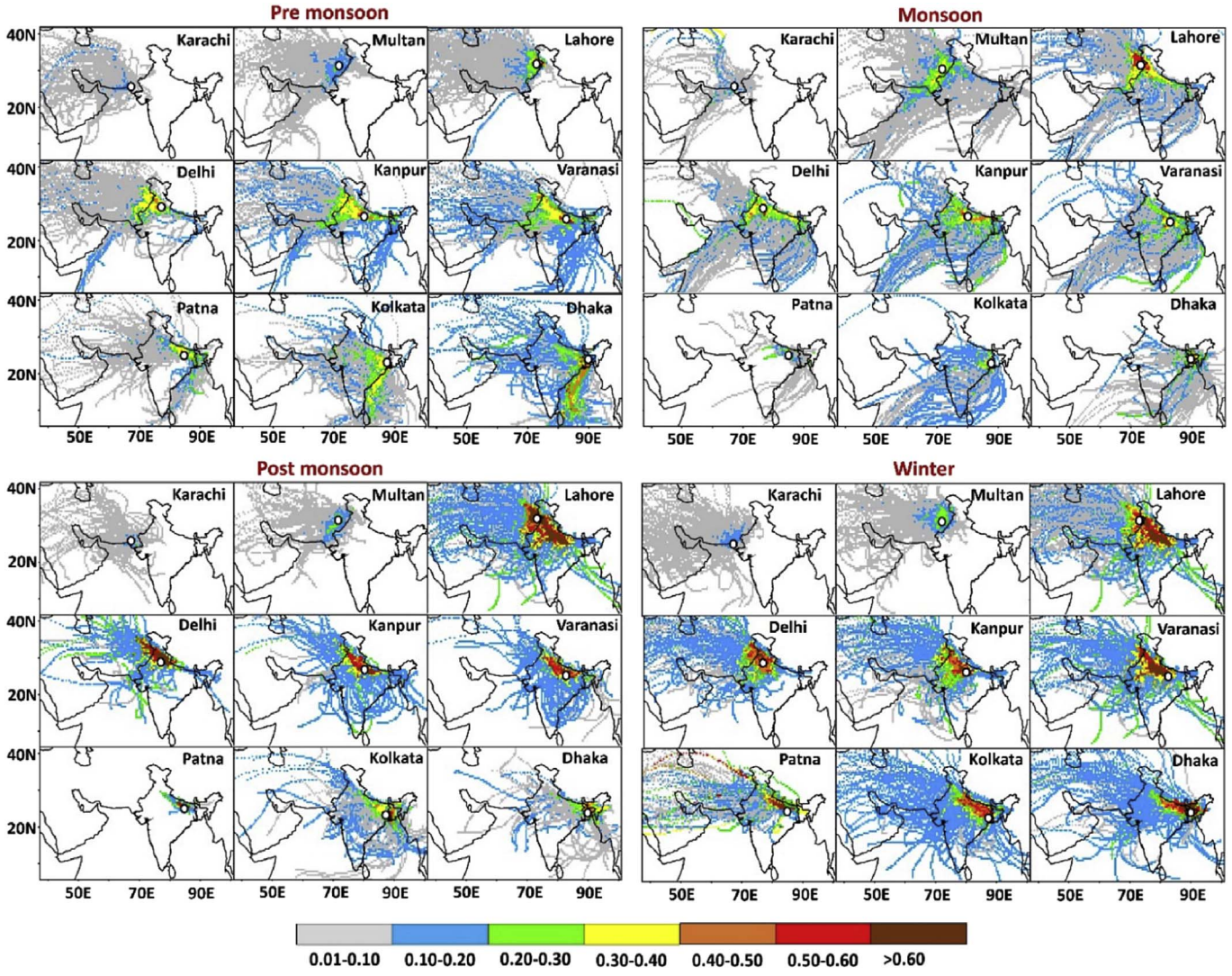

Fig. 9. The seasonal CWT map for AOD at all stations across IGP during 2006–2015.

based aerosol climatology over the Indo-Gangetic Plain highlights some key findings on long-term aerosol properties, its trends, current rate of change, and forecasting with future aerosol loading scenario. The most important findings of the study include the footprint of the highly heterogeneous spatio-temporal characteristics of the aerosols, spatially variable trends in its growth as well as the existence of a variety of aerosol source regions. Some specific findings are:

The long-term spatial analysis identifies a region of aerosol pool in the eastern part of IGP with exceptionally high aerosol load. Overall, stations located at the central and lower IGP are characterized with high aerosol loading while comparatively low AOD are noted over stations at upper part.

We evaluate the spatial and seasonal pattern of the trends across IGP and quantify in terms of changes in AOD and particle size. A sharp variation in aerosol types is noted over different regions, with the upper IGP mainly dominate by coarser particles, while the central and lower IGP exhibit the dominance of mixed and fine aerosols.

The spatial inconsistencies in the distribution of aerosol types is primarily attributed to seasonal variations in particle source strength and to regional meteorology. Further, aerosol hotspots are not always associated with urban centres but translates across the region.

Within the last decade, the monotonic trend in aerosol loadings reveals a uniform positive trend (i.e. increasing AOD), with different level of significance.

ARIMA-based forecasting of AOD indicates spatial variations in the model performance. A better suitability of ARIMA-based prediction is noted over central IGP compared to stations at upper and lower IGP. Such predictions may be important for forecasting future aerosol levels across IGP, where there is paucity of ground observation facility.

Concentration weighted trajectories over individual stations depict diverse aerosol source regions that contribute to the aerosol burden. During post-monsoon and winter, local sources are mostly dominated for majority of stations. In contrast, during summer, relatively distant sources add coarser particulates to the upper and central IGP. Aerosol profile during monsoon is primarily governed by coarse sea salt and mixed continental aerosols facilitated by monsoonal wind.

Acknowledgements

Present submission is supported by Department of Science and Technology, New Delhi (SR/FTP/ES-52/2014). MK acknowledge the Council for Scientific and Industrial Research (CSIR) for Senior Research Fellowship. AM acknowledges the Jawaharlal Nehru Scholarship from Jawaharlal Nehru Memorial Fund (JNMF), New Delhi for Doctoral studies. The Terra MODIS data is courtesy of NASA's Earth-Sun System Division. Authors acknowledge the NOAA-ARL for HYSPLIT model and NCEP/NCAR Reanalysis team for providing synoptic meteorological maps. Authors also acknowledge the R open access software package.

Appendix A. Supplementary data

Supplementary data related to this article can be found at http://dx.doi.org/10.1016/j.atmosenv.2018.02.027.

The symbols +, *, ** and *** indicate the level-of-significance at $p < 0.1$, $p < 0.01$, $p < 0.001$ and $p < 0.0001$.

References

Abish, B., Mohanakumar, K., 2013. Absorbing aerosol variability over the Indian subcontinent and its increasing dependence on ENSO. Global Planet. Change 106, 13–19.
Alam, K., Trautmann, T., Blaschke, T., 2011. Aerosol optical properties and radiative forcing over mega-city Karachi. Atmos. Res. 101 (3), 773–782.
Altaratz, O., Bar-Or, R.Z., Wollner, U., Koren, I., 2013. Relative humidity and its effect on aerosol optical depth in the vicinity of convective clouds. Environ. Res. Lett. 8 (3) 034025.
Banerjee, T., Kumar, M., Mall, R.K., Singh, R.S., 2017. Airing 'clean air' in clean India mission. Environ. Sci. Pollut. Control Ser. 24 (7), 6399–6413.
Banerjee, T., Murari, V., Kumar, M., Raju, M.P., 2015. Source apportionment of airborne particulates through receptor modeling: Indian scenario. Atmos. Res. 164, 167–187.
Begum, B.A., Hopke, P.K., Markwitz, A., 2013. Air pollution by fine particulate matter in Bangladesh. Atmospheric Pollution Research 4 (1), 75–86.
Bennouna, Y.S., Cachorro, V., Burgos, M.A., Toledano, C., Torres, B., de Frutos, A., 2014. Relationships between columnar aerosol optical properties and surface particulate matter observations in north-central Spain from long-term records (2003-2011). Atmospheric Measurement Techniques Discussions 7, 5829–5882.
Bilal, M., Nichol, J.E., 2015. Evaluation of MODIS aerosol retrieval algorithms over the Beijing-Tianjin-Hebei region during low to very high pollution events. J. Geophys. Res.: Atmosphere 120 (15), 7941–7957.
Bilal, M., Nichol, J.E., Nazeer, M., 2016. Validation of Aqua-MODIS C051 and C006 operational aerosol products using AERONET measurements over Pakistan. IEEE Journal of Selected Topics in Applied Earth Observations and Remote Sensing 9 (5), 2074–2080.
Burney, J., Ramanathan, V., 2014. Recent climate and air pollution impacts on Indian agriculture. Proc. Natl. Acad. Sci. Unit. States Am. 111 (46), 16319–16324.
Dey, S., Di Girolamo, L., 2011. A decade of change in aerosol properties over the Indian subcontinent. Geophys. Res. Lett. 38 (14).
Dey, S., Tripathi, S.N., Singh, R.P., Holben, B.N., 2004. Influence of dust storms on the aerosol optical properties over the Indo-Gangetic basin. J. Geophys. Res.: Atmosphere 109 (D20).
Di Girolamo, L., Bond, T.C., Bramer, D., Diner, D.J., Fettinger, F., Kahn, R.A., Rasch, P.J., 2004. Analysis of Multi-angle Imaging SpectroRadiometer (MISR) aerosol optical depths over greater India during winter 2001–2004. Geophys. Res. Lett. 31 (23).
Draxler, R.R., Hess, G.D., 1998. An overview of the HYSPLIT_4 modelling system for trajectories. Aust. Meteorol. Mag. 47 (4), 295–308.
Evans, J., van Donkelaar, A., Martin, R.V., Burnett, R., Rainham, D.G., Birkett, N.J., Krewski, D., 2013. Estimates of global mortality attributable to particulate air pollution using satellite imagery. Environ. Res. 120, 33–42.
Fang, H., Liang, S., Hoogenboom, G., 2011. Integration of MODIS LAI and vegetation index products with the CSM–CERES–Maize model for corn yield estimation. Int. J. Rem. Sens. 32 (4), 1039–1065.
Gautam, R., Hsu, N.C., Tsay, S.C., Lau, K.M., Holben, B., Bell, S., Payra, S., 2011. Accumulation of aerosols over the Indo-Gangetic plains and southern slopes of the Himalayas: distribution, properties and radiative effects during the 2009 pre-monsoon season. Atmos. Chem. Phys. 11 (24), 12841–12863.
Giles, D.M., Holben, B.N., Tripathi, S.N., Eck, T.F., Newcomb, W.W., Slutsker, I., Singh, R.P., 2011. Aerosol properties over the Indo-Gangetic Plain: a mesoscale perspective from the TIGERZ experiment. J. Geophys. Res.: Atmosphere 116 (D18).
Gogoi, M.M., Moorthy, K.K., Kompalli, S.K., Chaubey, J.P., Babu, S.S., Manoj, M.R., Prabhu, T.P., 2014. Physical and optical properties of aerosols in a free tropospheric environment: results from long-term observations over western trans-Himalayas. Atmos. Environ. 84, 262–274.
Granadoz-Munoz, M.J., Pozo-Vazquez, D., Guerrero-Rascado, J.L., Alados-Arboledas, L., 2011. Study of aerosol optical properties over the Iberian Peninsula based on 9 year MODIS dataset. In: Proceedings of the Global Conference on Global Warming, Lisbon, Portugal.
Gupta, P., Khan, M.N., da Silva, A., Patadia, F., 2013. MODIS aerosol optical depth observations over urban areas in Pakistan: quantity and quality of the data for air quality monitoring. Atmospheric pollution research 4 (1), 43–52.
Han, S., Bian, H., Zhang, Y., Wu, J., Wang, Y., Tie, X., Yao, Q., 2012. Effect of aerosols on visibility and radiation in spring 2009 in Tianjin, China. Aerosol Air Qual. Res 12, 211–217.
He, L., Wang, L., Lin, A., Zhang, M., Bilal, M., Wei, J., 2018. Performance of the NPP-VIIRS and aqua-MODIS aerosol optical depth products over the yangtze river basin. Rem. Sens. 10 (1), 117.
Henriksson, S.V., Laaksonen, A., Kerminen, V.M., Räisänen, P., Järvinen, H., Sundström, A.M., Leeuw, G.D., 2011. Spatial distributions and seasonal cycles of aerosols in India and China seen in global climate-aerosol model. Atmos. Chem. Phys. 11 (15), 7975–7990.
Hsu, N.C., Jeong, M.J., Bettenhausen, C., Sayer, A.M., Hansell, R., Seftor, C.S., Tsay, S.C., 2013. Enhanced Deep Blue aerosol retrieval algorithm: the second generation. J. Geophys. Res.: Atmosphere 118 (16), 9296–9315.
Karar, K., Gupta, A.K., 2007. Source apportionment of PM10 at residential and industrial sites of an urban region of Kolkata, India. Atmos. Res. 84, 30–41.
Kaskaoutis, D.G., Gautam, R., Singh, R.P., Houssos, E.E., Goto, D., Singh, S., Holben, B.N., 2012. Influence of anomalous dry conditions on aerosols over India: transport, distribution and properties. J. Geophys. Res.: Atmosphere 117 (D9).
Kaufman, Y.J., Koren, I., Remer, L.A., Rosenfeld, D., Rudich, Y., 2005. The effect of smoke, dust, and pollution aerosol on shallow cloud development over the Atlantic Ocean. Proc. Natl. Acad. Sci. U.S.A. 102 (32), 11207–11212.
Kendall, M.G., 1975. Rank Correlation Methods: 10 Tab. Griffin).
Khwaja, H.A., Parekh, P.P., Khan, A.R., Hershey, D.L., Naqvi, R.R., Malik, A., Khan, K., 2009. An in-depth characterization of urban aerosols using electron microscopy and energy dispersive x-ray analysis. Clean–Soil, Air, Water 37 (7), 544–554.
Klingmüller, K., Pozzer, A., Metzger, S., Stenchikov, G.L., Lelieveld, J., 2016. Aerosol optical depth trend over the Middle East. Atmos. Chem. Phys. 16 (8), 5063–5073.
Krishna Moorthy, K., Suresh Babu, S., Manoj, M.R., Satheesh, S.K., 2013. Buildup of aerosols over the Indian region. Geophys. Res. Lett. 40 (5), 1011–1014.
Kumar, D.B., Verma, S., 2016. Potential emission flux to aerosol pollutants over Bengal Gangetic plain through combined trajectory clustering and aerosol source fields analysis. Atmos. Res. 178, 415–425.
Kumar, M., Raju, M.P., Singh, R.K., Singh, A.K., Singh, R.S., Banerjee, T., 2017a. Wintertime characteristics of aerosols over middle Indo-Gangetic Plain: vertical

profile, transport and radiative forcing. Atmos. Res. 183, 268–282.
Kumar, M., Raju, M.P., Singh, R.S., Banerjee, T., 2017b. Impact of drought and normal monsoon scenarios on aerosol induced radiative forcing and atmospheric heating rate in Varanasi over middle Indo-Gangetic Plain. J. Aerosol Sci. 113 95–10.
Kumar, M., Singh, R.K., Murari, V., Singh, A.K., Singh, R.S., Banerjee, T., 2016. Fireworks induced particle pollution: a spatio-temporal analysis. Atmos. Res. 180, 78–91.
Kumar, M., Singh, R.S., Banerjee, T., 2015a. Associating airborne particulates and human health: exploring possibilities: comment on: kim, Ki-Hyun, Kabir, E. and Kabir, S. 2015. A review on the human health impact of airborne particulate matter. Environ. Int. 74 (2015), 136–143 Environment international, 84, 201.
Kumar, M., Tiwari, S., Murari, V., Singh, A.K., Banerjee, T., 2015b. Wintertime characteristics of aerosols at middle Indo-Gangetic Plain: impacts of regional meteorology and long range transport. Atmos. Environ. 104, 162–175.
Li, C., McLinden, C., Fioletov, V., Krotkov, N., Carn, S., Joiner, J., Streets, D., He, H., Ren, X., Li, Z., Dickerson, R.R., 2017. India is overtaking China as the World's largest emitter of anthropogenic sulfur dioxide. Sci. Rep. 7 (1), 14304.
Li, J., Carlson, B.E., Dubovik, O., Lacis, A.A., 2014. Recent trends in aerosol optical properties derived from AERONET measurements. Atmos. Chem. Phys. 14 (22), 12271–12289.
Lodhi, N.K., Beegum, S.N., Singh, S., Kumar, K., 2013. Aerosol climatology at Delhi in the western Indo-Gangetic Plain: microphysics, long-term trends, and source strengths. J. Geophys. Res. Atmos. 118 (3), 1361–1375.
Maghrabi, A.H., Alotaibi, R.N., 2017. Long-term variations of AOD from an AERONET station in the central Arabian Peninsula. Theor. Appl. Climatol. 1–12.
Mann, H.B., 1945. Nonparametric tests against trend. Econometrica: J. Econom. Soc. 245–259.
Mao, K.B., Ma, Y., Xia, L., Chen, W.Y., Shen, X.Y., He, T.J., Xu, T.R., 2014. Global aerosol change in the last decade: An analysis based on MODIS data. Atmos. Environ. 94, 680–686.
Mhawish, A., Kumar, M., Mishra, A.K., Srivastava, P.K., Banerjee, T., 2018. Remote sensing of aerosols from space: retrieval of properties and applications. In: Remote Sensing of Aerosols, Clouds, and Precipitation. Publisher: Elsevier Inc, pp. 1–38. (. https://doi.org/10.1016/B978-0-12-810437-8.00003-7).
Mhawish, A., Banerjee, T., Broday, D.M., Misra, A., Tripathi, S.N., 2017. Evaluation of MODIS Collection 6 aerosol retrieval algorithms over Indo- Gangetic Plain: implications of aerosols types and mass loading. Rem. Sens. Environ. 201, 297–313.
Murari, V., Kumar, M., Mhawish, A., Barman, S.C., Banerjee, T., 2017. Airborne particulate in Varanasi over middle Indo-Gangetic Plain: variation in particulate types and meteorological influences. Environ. Monit. Assess. 189 (4), 157.
Murari, V., Kumar, M., Singh, N., Singh, R.S., Banerjee, T., 2016. Particulate morphology and elemental characteristics: variability at middle Indo-Gangetic Plain. J. Atmos. Chem. 73 (2), 165–179.
Pandey, A., Sadavarte, P., Rao, A.B., Venkataraman, C., 2014. Trends in multi-pollutant emissions from a technology-linked inventory for India: II. Residential, agricultural and informal industry sectors. Atmos. Environ. 99, 341–352.
Pandey, S.K., Vinoj, V., Landu, K., Babu, S.S., 2017. Declining pre-monsoon dust loading over South Asia: signature of a changing regional climate. Sci. Rep. 7 (1), 16062.
Pandithurai, G., Dipu, S., Dani, K.K., Tiwari, S., Bisht, D.S., Devara, P.C.S., Pinker, R.T., 2008. Aerosol radiative forcing during dust events over New Delhi, India. J. Geophys. Res. Atmos. 113 (D13).
Prasad, A.K., Singh, R.P., 2007. Changes in aerosol parameters during major dust storm events (2001–2005) over the Indo-Gangetic Plains using AERONET and MODIS data. J. Geophys. Res. Atmos. 112 (D9).
Ramachandran, S., Kedia, S., Srivastava, R., 2012. Aerosol optical depth trends over different regions of India. Atmos. Environ. 49, 338–347.
Rastogi, N., Patel, A., 2017. Oxidative potential of ambient aerosols: an Indian perspective. Curr. Sci. 112 (1), 35.
Reddy, M.S., Venkataraman, C., 2002. Inventory of aerosol and Sulphur dioxide emissions from India. Part II-biomass combustion. Atmos. Environ. 36, 699–712.
Sadavarte, P., Venkataraman, C., 2014. Trends in multi-pollutant emissions from a technology-linked inventory for India: I. Industry and transport sectors. Atmos. Environ. 99, 353–364.
Saud, T., Mandal, T.K., Gadi, R., Singh, D.P., Sharma, S.K., Saxena, M., Mukherjee, A., 2011. Emission estimates of particulate matter (PM) and trace gases (SO2, NO and NO2) from biomass fuels used in rural sector of Indo-Gangetic Plain, India. Atmos. Environ. 45, 5913–5923.
Schulz, M., Textor, C., Kinne, S., Balkanski, Y., Bauer, S., Berntsen, T., Isaksen, I.S.A., 2006. Radiative forcing by aerosols as derived from the AeroCom present-day and pre-industrial simulations. Atmos. Chem. Phys. 6 (12), 5225–5246.
Seinfeld, J.H., Bretherton, C., Carslaw, K.S., Coe, H., DeMott, P.J., Dunlea, E.J., Kraucunas, I., 2016. Improving our fundamental understanding of the role of aerosol − cloud interactions in the climate system. Proc. Natl. Acad. Sci. Unit. States Am. 113 (21), 5781–5790.
Sen, A., Abdelmaksoud, A.S., Ahammed, Y.N., Banerjee, T., Bhat, M.A., Chatterjee, A., Gadi, R., 2017. Variations in particulate matter over Indo-Gangetic Plains and Indo-Himalayan Range during four field campaigns in winter monsoon and summer monsoon: role of pollution pathways. Atmos. Environ. 154, 200–224.
Sen, A., Ahammed, Y.N., Banerjee, T., Chatterjee, A., Choudhuri, A.K., Das, T., Mandal, T.K., 2016. Spatial variability in ambient atmospheric fine and coarse mode aerosols over Indo-Gangetic plains, India and adjoining oceans during the onset of summer monsoons, 2014. Atmos. Pollut. Res. 7 (3), 521–532.
Shahid, M.Z., Hong, L., Yu-Lu, Q., Shahid, I., 2015. Source sector contributions to aerosol levels in Pakistan. Atmos. Ocean. Sci. Lett. 8 (5), 308–313.
Sharma, S.K., Kumar, M., Gupta, N.C., Saxena, M., Mandal, T.K., 2014. Characteristics of ambient ammonia over Delhi, India. Meteorol. Atmos. Phys. 124 (1–2), 67–82.
Sharma, S.K., Mandal, T.K., Saxena, M., 2017. Inter-annual variation of ambient ammonia and related trace gases in Delhi, India. Bull. Environ. Contam. Toxicol. 99 (2), 281–285.
Shohel, M., Kistler, M., Rahman, M.A., Kasper-Giebl, A., Reid, J.S., Salam, A., 2017. Chemical characterization of PM2. 5 collected from a rural coastal island of the Bay of Bengal (Bhola, Bangladesh). Environ. Sci. Pollut. Control Ser. 1–12.
Singh, N., Mhawish, A., Deboudt, K., Singh, R.S., Banerjee, T., 2017b. Organic aerosols over Indo-Gangetic Plain: sources, distributions and climatic implications. Atmos. Environ. 157, 59–74.
Singh, N., Murari, V., Kumar, M., Barman, S.C., Banerjee, T., 2017a. Fine particulates over South Asia: review and meta-analysis of PM 2.5 source apportionment through receptor model. Environ. Pollut. 223, 121–136.
Soni, K., Kapoor, S., Parmar, K.S., Kaskaoutis, D.G., 2014. Statistical analysis of aerosols over the Gangetic–Himalayan region using ARIMA model based on long-term MODIS observations. Atmos. Res. 149, 174–192.
Soni, K., Parmar, K.S., Kapoor, S., 2015. Time series model prediction and trend variability of aerosol optical depth over coal mines in India. Environ. Sci. Pollut. Control Ser. 22 (5), 3652–3671.
Sorek-Hamer, M., Cohen, A., Levy, R.C., Ziv, B., Broday, D.M., 2013a. Classification of dust days by satellite remotely sensed aerosol products. Int. J. Rem. Sens. 34 (8), 2672–2688.
Sorek-Hamer, M., Kloog, I., Koutrakis, P., Strawa, A.W., Chatfield, R., Cohen, A., Broday, D.M., 2015. Assessment of PM 2.5 concentrations over bright surfaces using MODIS satellite observations. Rem. Sens. Environ. 163, 180–185.
Sorek-Hamer, M., Strawa, A.W., Chatfield, R.B., Esswein, R., Cohen, A., Broday, D.M., 2013b. Improved retrieval of PM 2.5 from satellite data products using non-linear methods. Environ. Pollut. 182, 417–423.
Srinivas, B., Sarin, M.M., 2014. PM 2.5, EC and OC in atmospheric outflow from the Indo-Gangetic Plain: temporal variability and aerosol organic carbon-to-organic mass conversion factor. Sci. Total Environ. 487, 196–205.
Srivastava, A., Saran, S., 2017. Comprehensive study on AOD trends over the Indian subcontinent: a statistical approach. Int. J. Rem. Sens. 38 (18), 5127–5149.
Streets, D.G., Yan, F., Chin, M., Diehl, T., Mahowald, N., Schultz, M., Yu, C., 2009. Anthropogenic and natural contributions to regional trends in aerosol optical depth, 1980–2006. J. Geophys. Res. Atmos. 114 (D10).
Tao, M., Chen, L., Wang, Z., Tao, J., Che, H., Wang, X., Wang, Y., 2015. Comparison and evaluation of the MODIS Collection 6 aerosol data in China. J. Geophys. Res. Atmos. 120 (14), 6992–7005.
Van Donkelaar, A., Martin, R.V., Brauer, M., Kahn, R., Levy, R., Verduzco, C., Villeneuve, P.J., 2010. Global estimates of ambient fine particulate matter concentrations from satellite-based aerosol optical depth: development and application. Environ. Health Perspect. 118 (6), 847.
Warner, J.X., Dickerson, R.R., Wei, Z., Strow, L.L., Wang, Y., Liang, Q., 2017. Increased atmospheric ammonia over the world's major agricultural areas detected from space. Geophys. Res. Lett. 44 (6), 2875–2884.
Wei, J., Sun, L., Huang, B., Bilal, M., Zhang, Z., Wang, L., 2018. Verification, improvement and application of aerosol optical depths in China Part 1: inter-comparison of NPP-VIIRS and Aqua-MODIS. Atmos. Environ. 175, 221–233.
Yuval and Broday, D.M., 2010. Studying the time scale dependence of environmental variables predictability using fractal analysis. Environ. Sci. Technol. 44 (12), 4629–4634.
Zhao, B., Jiang, J.H., Gu, Y., Diner, D., Worden, J., Liou, K.N., Huang, L., 2017. Decadal-scale trends in regional aerosol particle properties and their linkage to emission changes. Environ. Res. Lett. 12 (5) 054021.